Biophysical Journal Volume 100 April 2011 1855–1863

A Few Immobilized Thrombins Are Sufficient for Platelet Spreading

Yosuke Okamura,[†] Roman Schmidt,[‡] Ines Raschke,[†] Maik Hintze,[†] Shinji Takeoka,[§] Alexander Egner,[‡] and Thorsten Lang[†*]

[†]Membrane Biochemistry, Life and Medical Sciences (LIMES) Institute, University of Bonn, Bonn, Germany; [‡]Department of NanoBiophotonics, Max Planck Institute for Biophysical Chemistry, Göttingen, Germany; and [§]Department of Life Science and Medical Bioscience, Graduate School of Advanced Science and Engineering, Waseda University, TWIns, Tokyo, Japan

ABSTRACT Eukaryotic cells respond to signaling molecules with picomolar to nanomolar sensitivities. However, molar concentrations give no suggestion of the sufficient number of molecules per cell and are confusing when referring to physiological situations in which signaling molecules act in an immobilized state. Here, we studied platelet adhesion by thrombin, a key step in normal hemostasis and pathological arterial thrombosis. We generated a biofunctional nanosheet surface to mimic the in vivo solid-state interaction between platelets and thrombin at sites of injured tissues. We observed that <10 molecules readily activate platelets with high specificity, resulting in platelet adhesion and spreading. This number is much lower than expected from previous experiments in solution, in which the sole activation of platelets required a >1000-fold stoichiometric excess of thrombin. We conclude that immobilizing thrombin apposed to the membrane receptor allows platelets to respond with very high sensitivity. Moreover, we propose that irreversible cell activation may require several ligands to avoid activation by single, mislocalized signaling molecules.

INTRODUCTION

Organisms respond to signal-triggering molecules with impressively high sensitivities in the nanomolar or even picomolar concentration range (1,2). At concentrations of several picomolar, one molecule occupies a volume equivalent to the size of a small cell, which intuitively suggests that only a few molecules may be sufficient for activation. However, more important than the molecular density seen by the cell is the number of effective molecules, which depends on the binding affinity of the signaling molecule to the receptor, the receptor density, the incubation time, and whether the fraction of activated receptors can produce a sufficiently strong intracellular signal. These issues make it difficult to predict the number of necessary molecules from a given concentration associated with cell activation. Therefore, estimates have been obtained for only a few cases; for example, Ueda and Shibata (3) reported that several thousand receptors per cell are occupied during picomolar-sensitive chemotaxis.

Although activating concentrations are already difficult to interpret, the situation becomes even more complex when ligands become immobilized before they interact with receptors. One such example is the activation of platelets by thrombin, a key step in normal hemostasis and pathological arterial thrombosis (4,5) resulting in platelet adhesion, spreading, and aggregation. A concentration of 0.5 nM thrombin (6) has been reported to be associated with the transition from the nonactivated to the activated state when platelets and thrombin are incubated in solution, corresponding to a thrombin/platelet ratio of ~1200:1. However, for adhesion under physiological conditions, a variety of mechanisms recruit platelets from the bloodstream and immobilize them at sites of vascular injuries (7). Such sites are marked by exposed basal laminal collagen from the subendothelial matrix, to which platelets bind directly or indirectly via glycoprotein (GP) surface receptors. At this stage, thrombin interacts with platelets not only in solution but also in a solid-state configuration in which thrombin is immobilized at the subendothelial matrix (8) and the surface of activated endothelial cells (9). In addition, thrombin may be directly involved in platelet recruitment by binding to the platelet surface receptor GPIbα (10). Once the thrombin molecules and platelets are closely apposed to each other, thrombin triggers platelet activation by switching on G-protein coupled receptors from the protease activated receptor (PAR) family. To this end, thrombin cleaves PAR-1 (and also PAR-4), producing a new receptor N-terminus that intramolecularly binds to the ligand-binding site, representing a receptor locked in the on state (11).

Under these conditions, the concentration required for activation would be best described by a surface concentration or a defined number of immobilized thrombin molecules per apposed platelet. To determine this number, we set up an assay system in which platelets were allowed to establish contact with a thrombin-coated surface (12). For stable thrombin adsorption, we turned to free-standing hydrophobic poly-L-lactic acid (PLLA) nanosheets with a thickness of 60 nm (13), which for microscopic analysis were attached to glass coverslips without any adhesive reagent. PLLA nanosheets provide a hydrophobic surface to which proteins can stably adsorb by hydrophobic interactions. Moreover, they

Submitted October 6, 2010, and accepted for publication February 28, 2011.

*Correspondence: thorsten.lang@uni-bonn.de

Alexander Egner's present address is Department of Optical Nanoscopy, Laser Laboratory Göttingen e.V., Göttingen, Germany.

Editor: Jason M. Haugh.

0006-3495/11/04/1855/9 $2.00

doi: 10.1016/j.bpj.2011.02.052

do not disturb microscopic analysis by fluorescence, they provide an inert surface that cannot trigger unspecific platelet activation, and they can be removed again from the coverslip to analyze the amount and activity of the adsorbed protein.

MATERIALS AND METHODS

Preparation of nanosheets

We prepared 60-nm-thick PLLA nanosheets essentially as described previously (13). First, to produce a water-soluble sacrificial layer, we pipetted an aqueous solution of 10 mg/ml polyvinyl alcohol (PVA, molecular mass 22 kDa, 99% hydrolyzed; Kanto Chemical, Tokyo, Japan) onto 4 cm × 4 cm SiO_2 wafers (P-type Si (100) wafers covered with thermally grown silicon oxide (SiO_2); KST World, Fukui, Japan). The wafers were spin-coated at 4000 rpm (spin coater IH-D3; Mikasa Ltd., Tokyo, Japan) for 20 s and then dried at 70°C for 90 s. Using the same procedure, we then coated the PVA-coated SiO_2 wafers with 10 mg/ml PLLA in methylene chloride (molecular mass 80–100 kDa; Polysciences, Warrington, PA). Next, we detached the PLLA nanosheets from the wafers by dissolving the PVA sacrificial layer with water and picked up the floating nanosheets with a glass coverslip (25 mm diameter for adhesion studies, and 12 mm for experiments in which fluorescent nanosheets were imaged), forming a coverslip with a tightly attached nanosheet. Finally, the preparation was dried overnight at 70°C.

Detachable nanosheets were prepared by sandwiching a water-soluble sacrificial PVA layer between the PLLA nanosheets and the coverslips. To this end, 12-mm-diameter coverslips were directly coated with PVA followed by PLLA coating.

Protein-nanosheet adsorption

The thrombin solutions used for coating contained thrombin or fluorescent-labeled thrombin in phosphate-buffered saline (PBS; 2.7 mM KCl, 1.5 mM KH_2PO_4, 137 mM NaCl, 8.1 mM Na_2HPO_4, pH 7.4) at a concentration as indicated (referring to units as quoted by the supplier; bovine thrombin, catalog No. T4648, lot No. 025K76356; Sigma-Aldrich, Saint Louis, MO). For fluorescent labeling of the thrombin solution, we used tetramethyl-rhodamine iso-thio-cyanate (TRITC, catalog No. T2639; Sigma-Aldrich), adding 5–20 μl of 10 mM TRITC in DMSO to 1 ml of a 100 U/ml thrombin solution in PBS. The mixture was incubated for 1 h at room temperature (RT) and the nonreacted dye was separated from the protein by gel filtration using a Sephadex G25 column (GE Healthcare UK, Buckinghamshire, UK).

For coating, the thrombin solutions were pipetted directly onto the nanosheets (100 μl and 500 μl were applied to 12- and 25-mm-diameter coverslips, respectively) and incubated overnight at 4°C. For the adhesion studies, 10 U/ml of thrombin coating were applied overnight or for at least for 3 h (no difference in adhesion was observed). Finally, the coverslips were carefully rinsed three times with PBS and incubated with 3% (w/v) bovine serum albumin (BSA; Sigma-Aldrich) in PBS at 4°C for 2 h (this step was omitted in experiments using detachable nanosheets or when fluorescent-labeled sheets on a coverslip were imaged). We evaluated the stability of the thrombin adsorption by using a coating of 0.1 U/ml TRITC-labeled thrombin. After coating was completed, we performed one to six 5-min washing steps and analyzed the average fluorescence intensity by fluorescence microscopy. The results showed no significant loss of protein during a total washing period of 30 min (data not shown).

Platelet adhesion assay

We added 10% (v/v) of a 3.8% (w/v) sodium citrate solution to blood drawn from healthy volunteers after they provided written informed consent according to the guidelines of the institutional review board of the University of Bonn. An initial centrifugation step (120 × *g*, 15 min, 22°C) yielded platelet-rich plasma in the supernatant, to which a 15% volume of an acid-citrate-dextrose solution (2.2% (w/v) sodium citrate, 0.8% (w/v) citric acid, 2.2% (w/v) glucose, and 2 μM prostaglandin E_1 (PGE_1, catalog No. P5515; Sigma-Aldrich)) was added. After centrifugation (1500 × *g*, 7 min, 22°C), the platelets were resuspended in Ringer's citrate-dextrose solution (0.76% (w/v) citric acid, 0.090% (w/v) glucose, 0.043% (w/v) $MgCl_2$, 0.038% (w/v) KCl, 0.60% (w/v) NaCl, 2 μM PGE_1, pH 6.5) and spun down again (1500 × *g*, 7 min, 22°C). The remaining pellet was resuspended in HEPES-Tyrode buffer (5.6 mM glucose, 2.7 mM KCl, 1 mM $MgCl_2$, 137 mM NaCl, 12 mM $NaHCO_3$, 0.4 mM NaH_2PO_4, 10 mM HEPES, pH 7.4) containing 1 mM $CaCl_2$, with the concentration adjusted to 2.0×10^5 platelets/μl for the platelet adhesion assay.

To test whether the platelets were already activated after purification, we analyzed the amount of P-selectin that mobilized to the cell surface. After purification, 50 μl suspensions of 1.0×10^5 platelets/μl were incubated at 37°C for up to 90 min. As a positive control, one suspension was incubated for 10 min with the addition of 0.25 U/ml thrombin. Then 0.13 μg FITC-labeled mouse anti-human P-selectin antibody (catalog No. 555523; BD Biosciences, San Diego, CA) or FITC-labeled mouse IgG κ isotype control (catalog No. 555748; BD Biosciences), as a control for unspecific antibody binding, were added followed by a 5 min incubation at RT and fixation by formaldehyde (1.5% (v/v)). Platelets were gated to their characteristic forward versus side scatter. We then measured the fraction of positive cells in 10,000 platelets using fluorescence-activated cell sorting (FACSCanto II flow cytometer; BD Biosciences, San Jose, CA) and analyzed the results with FlowJo software (TreeStar, Ashland, OR).

For the adhesion experiments, 500 μl platelet suspensions were transferred onto coverslip adsorbed nanosheets that were incubated in six-well plates for various time periods as indicated, and maintained at 37°C with a water bath. Where indicated, before the platelets were incubated with the nanosheets, platelets in HEPES-Tyrode buffer (containing 1 mM $CaCl_2$) and/or nanosheets in PBS were treated with the following reagents: Hirudin (recombinant hirudin from yeast, catalog No. 94581; Sigma-Aldrich), *N*3-cyclopropyl-7-[[4-(1-methylethyl) phenyl]methyl]-7*H*-pyrrolo [3,2-*f*]quinazoline-1,3-diamine dihydrochloride (SCH79797; catalog No. 1592; Tocris Bioscience, Ellisville, MO; SCH79797 was dissolved in DMSO and in the corresponding control condition the buffer also contained DMSO), D-Phe-L-Pro-L-Arg chloromethyl ketone dihydrochloride (PPACK, catalog No. 520222; Merck KGaA, Darmstadt, Germany), anti-GPIbα monoclonal antibody (SZ2; Beckman Coulter, Brea, CA), RGDS peptide (catalog No. A9041; Sigma-Aldrich), or ReoPro (license number for Germany 100a/94, manufactured by Centocor B.V., Leiden, The Netherlands). We washed off nonadherent platelets at RT by gently adding several milliliters of PBS, and further rinsed the coverslips two times with PBS. The cells were then fixed with 4% (w/v) paraformaldehyde (PFA) in PBS at 4°C for 90 min, quenched with 50 mM NH_4Cl in PBS at RT for 10 min, and washed three times with PBS for 5 min each.

In some experiments, samples were also immunostained for GPIIb to obtain additional information for the identification of platelets. To this end, platelets were permeabilized with Triton X-100 in PBS at RT for 10 min (using 0.5% Triton for Fig. 2 and Fig. S3 in the Supporting Material), and incubated at RT for 45 min with monoclonal mouse anti-human GPIIb antibody (catalog No. 555466; BD Biosciences) diluted 1:100 in 3% (w/v) BSA-PBS containing Triton X-100 (0.2% for Fig. 2 and Fig. S3). Subsequently, the cells were rinsed three times in PBS for 10 min each, followed by a 45 min incubation with a secondary antibody diluted in 3% BSA-PBS containing Triton X-100 (0.2% for Fig. 2 and Fig. S3). We used 1:200 diluted Alexa594 labeled donkey-anti-mouse (A21203, Invitrogen, Eugene, OR) for Fig. S3, and 1:50 diluted KK114-conjugated sheep anti-mouse IgG (obtained from the Department of NanoBiophotonics, Max Planck Institute for Biophysical Chemistry, Göttingen, Germany) for Fig. 2. The coverslips were washed three times in PBS for 10 min each. For stimulated emission depletion (STED) microscopy, samples were shipped in 4% PFA in PBS to the Max Planck Institute for Biophysical Chemistry.

Epifluorescence microscopy

For epifluorescence imaging, we used a total internal reflection fluorescence (TIRF) microscope (based on a motorized Olympus IX81 microscope; Olympus, Tokyo, Japan) equipped with an EMCCD camera (ImagEM C9100-13; Hamamatsu Photonics, Hamamatsu, Japan), a 488 nm laser, and a 150 W Xenon lamp integrated into the MT20-I-fluorescence illumination system. We used the microscope in epifluorescence mode by applying a 60× NA 1.49 Apochromat objective in combination with a 2× magnifying lens. For fluorescence excitation, the Xenon lamp was used at 100% intensity, and the Olympus filter set U-M3DAFIC3/HC was used for *N,N,N*-tri-methyl-4-(6-phenyl-1,3,5-hexa-trien-1-yl) phenyl-ammonium *p*-toluene-sulfonate (TMA-DPH; Sigma-Aldrich) and Alexa594 detection. The exposure times were 200 ms for Alexa594 and 1 s for TMA-DPH.

Imaging was performed in PBS containing TMA-DPH to visualize phospholipid membranes. For each condition, we recorded three to six images and analyzed the surface covered by activated platelets using the TMA-DPH image as reference. To this end, images were manually thresholded in Image J (National Institutes of Health, Bethesda, MD), and the area covered by platelets divided by the total image area yielded the percentage of area covered by platelets. For each condition, values obtained from individual images were averaged. In some experiments, using inverted images we also manually counted the number of platelets per field of view.

Quantification of adsorbed protein

Detachable PLLA nanosheets on 12-mm coverslips were coated with TRITC-labeled thrombin solutions as indicated. The supernatants were collected and coverslips were carefully rinsed three times with PBS. An incision at the edge of the coverslips was made with tweezers to facilitate the nanosheet detachment in PBS containing 1% sodium dodecyl sulfate (SDS; Carl-Roth GmbH, Karlsruhe, Germany). The detached nanosheets were transferred into 96-well plates, and fluorescence (E_x = 540 nm, E_m = 580 nm) was measured with a spectrophotometer (Infinite 200; Tecan Group Ltd., Männedorf, Switzerland). We determined the amount of total adsorbed protein by referring to calibration measurements with TRITC-labeled thrombin solutions containing in addition uncoated nanosheets and 1% SDS in PBS. In addition, we measured the loss of protein from the coating solution. To this end, we diluted the labeled protein with 1% SDS in PBS to the corresponding coating concentrations and measured it to obtain the value before coating. After coating was completed, the supernatants were diluted 1:10 and 1:100 with 1% SDS in PBS and measured. The values were corrected for evaporation that occurred during overnight incubation, yielding the amount of protein in the coating solution after coating. Subtraction of both values yielded the amount of protein lost from the coating solution. For one individual experiment, the two values (i.e., the amount on the nanosheet and the amount of lost protein) were averaged and used for plotting.

Imaging of fluorescent protein-coated nanosheets

Nanosheets on 12-mm-diameter coverslips with no sacrificial layer were coated with a 0.26 U/ml TRITC-labeled thrombin solution. For imaging, the coverslips carrying the nanosheets were placed on larger coverslips (25 mm diameter) mounted in a microscopy chamber that was filled with PBS. For imaging, we used an Olympus IX81 microscope (see above) applying a 10 × 0.4 NA Apochromat objective in the epifluorescence mode. We used the Xenon lamp at 100% intensity for fluorescence excitation, and the Olympus filter set U-M3DAFIC3/HC for TRITC detection. The exposure time was 200 ms and the camera gain was set to one. Images were taken from the periphery of the nanosheets. From each nanosheet, two to eight images were taken for analysis, and five to 10 values per image were determined for the inner and rim areas. To determine the width of the rim, we analyzed 15 linescans per nanosheet. Images were analyzed with the use of Image J software (National Institutes of Health).

SDS-PAGE

Samples together with BSA standards in 1.6% SDS were subjected to 12% (w/v) nonreducing SDS-PAGE. Polyacrylamide gels were stained with colloidal Coomassie. Fluorescence of the Coomassie dye induced by protein binding (14,15) was excited by a solid-state diode laser at 680 nm using the Odyssey Infrared Imaging System (Li-Cor Biosciences), which was also used for quantitation of the band intensities.

Mass spectrometry of excised bands was performed by the Proteomics Facility of the Cluster of Excellence, Cellular Stress Responses in Aging-Associated Diseases, University of Cologne (Cologne, Germany).

Activity of adsorbed thrombin

Thrombin activities were assayed in 150 mM imidazole buffer (pH 7.0) using N-(p-tosyl)-Gly-Pro-Arg-p-nitroanilide acetate salt (catalog No. T1637; Sigma-Aldrich) as a chromogenic substrate of thrombin. In addition, the assay buffer contained 0.01% Tween 20 to avoid nanosheet flotation. For analysis of thrombin activity in solution, 290 μl buffer aliquots in a 96-well plate contained substrate concentrations ranging from 0.031 to 1.0 mM or no substrate. After 10 min preincubation at 32°C, the reaction was initiated by addition of 10 μl thrombin protein solution (corresponding to 601 ng). To measure the activity of thrombin in the coated state, 300 μl buffer aliquots were incubated in 96-well plates and the reaction was initiated by adding the detached nanosheet (coated with 327 ng protein, as determined from Fig. 4). Under both assay conditions, the change in A_{405} was continuously monitored with the use of a spectrophotometer (Infinite 200) at 32°C. For each substrate concentration (S) the slope of the initial trace (velocity of product formation = V; an absorption coefficient of 4-nitroanilide 9500 M^{-1} cm^{-1} was used) was determined, 1/V was plotted versus 1/S, and a linear regression line was fitted. The point of intersection of the regression line with the *y* axis yielded $1/V_{max}$, and V_{max} was used as a reference for thrombin activity.

isoSTED microscopy

When the samples arrived at the Max Planck Institute for Biophysical Chemistry (Göttingen, Germany), the PFA was quenched for 10 min at RT by a PBS solution containing 50 mM NH_4Cl. For isoSTED imaging (16), the PBS buffer was exchanged by a dilution series with 2,2′-thiodiethanol in PBS (17), resulting in an embedding medium of 97% (v/v) 2,2′-thiodiethanol in PBS. The sample was covered with a second coverslip that was sparsely coated with fluorescent beads (crimson fluorescent microspheres, specified diameter 100 nm; Molecular Probes, Eugene, OR) to facilitate the initial alignment of the isoSTED microscope. Excitation at a wavelength of 635 nm was performed with a pulsed semiconductor laser (PDL 800-B with LDH-P-C 635b; PicoQuant, Berlin, Germany) that delivered <100 ps excitation pulses synchronized with STED pulses of ~1 ns length. The source of the STED light was a frequency-doubled fiber laser (ELP-5-775-DG; IPG Photonics, Oxford, MA) operating at 20 MHz and a wavelength of 775 nm. The time-averaged STED power in the sample was ~100 mW. The emission of the fluorophore KK114 was detected in the 660–700 nm wavelength range with the use of a photon-counting avalanche photodiode (PerkinElmer, Waltham, MA).

To analyze cluster size and density, we recorded images using a spherical point spread function and exported, rescaled, and filtered them with the blur filter (10%) in MetaMorph (Universal Imaging, West Chester, PA). We then cut out representative 100 × 100 pixel areas of 1.42 μm × 1.42 μm from the image of the cells. We identified individual clusters in these areas using

a custom-made program and calculated the average density as the number of identified clusters divided by the area. We then fitted each cluster with a Gaussian, taking into account a homogeneous background. We rejected fits that showed either a background of >10 photons or a center that deviated >21.3 nm from the initial guess of the cluster's center. The signal/noise ratios varied largely between the different experiments and we observed a trend toward smaller clusters at lower signal/noise ratios. To avoid underestimating the cluster size, we present the data from the experiment with the highest signal/noise ratio, from which 12 cells from four recordings were analyzed. In this set of experiments, we identified a total of 814 clusters from 12 cells. From 376 clusters, we obtained the size by fitting a Gaussian (in this case, fitting was repeated on unfiltered raw data). The cluster size and density are given as the mean ± standard deviation (SD; $n = 12$ cells).

To acquire an *xz* scan of the platelets (see Fig. 2, *upper panel*), we configured the point spread function of the microscope into an oblate shape (18). We then nonlinearly deconvolved the recorded data by applying 30 iterations of the Richardson-Lucy algorithm (19) to account for blurring effects of the imaging system.

TIRF microscopy

For measurement of the platelet contact area, platelets were settled down onto nanosheets coated overnight at 4°C with 3% BSA in PBS. Cells were incubated for 10 min at 37°C and then fixed with 4% (w/v) PFA in PBS at 4°C for 90 min. PFA was quenched at RT by gentle addition of a 10% volume of PBS containing 500 mM NH_4Cl for 10 min. Then the coverslips were mounted in a microscopy chamber and platelets were imaged in the presence of 5 μM *N*-(3-tri-ethyl-ammonium-propyl)-4-(4-(di-butyl-amino)-styryl)-pyridinium di-bomide (FM1-43; Invitrogen) in PBS to visualize their membranes. For imaging, we used a TIRF microscope (using a 60× NA 1.49 Apochromat objective in combination with a 2× and 1.6× magnifying lens; see above). We used a 488 nm laser line for TIRF illumination at 100% intensity in combination with Olympus filter U-MTIR488-HC. For epifluorescence, we used a Xenon lamp at 100% intensity with Olympus filter U-M3DAFIC3/HC. We first imaged the fields of view using epifluorescence and then acquired an image under TIRF illumination. For image analysis, we used the program Corel-Draw. Using the epifluorescence image as reference, we identified the contact areas in the TIRF image, outlined them manually, and determined their size using Image J with a TIFF image exported from Corel-Draw. Contact areas from spontaneously activated platelets were not included. For each coverslip, we recorded five to seven images. Two to four of these images were then used for analysis. Three independent experiments were performed.

RESULTS AND DISCUSSION

First, we tested whether thrombin-coated nanosheets indeed represent functionalized surfaces that can trigger specific platelet adhesion and spreading. At physiological temperature, purified platelets were allowed to settle down onto nanosheets coated with 10 U/ml thrombin and washed off after variable times, leaving attached platelets that underwent adhesion. As shown in Fig. 1 *A*, shortly after incubation we observed platelets with filopodial and lamellipodial extensions, representing intermediate states on the pathway to full spreading. The extent of platelet adhesion was time-dependent, and the process was completed in 10 min, when maximal surface coverage by fully spread platelets was achieved (Fig. 1, *A* and *B*). To exclude cell priming before incubation with nanosheets, we used fluorescence-activated cell sorting to determine whether P-selectin had been mobilized from α-granules to the cell surface. P-selectin on the surface of purified platelets incubated for variable times was fluorescently labeled by antibodies, and the percentage of positive cells was determined. As presented in Fig. S1, after 60 min a very minor percentage (~0.7%) of the platelets were positive for surface P-selectin, excluding platelet activation at the moment they were added to the nanosheets, which was either directly after purification or after a maximal 15 min pretreatment (e.g., Fig. 1 *E*).

We then sought to determine whether platelets adhere and spread specifically due to thrombin activation, and which adhesion molecule is involved in the adhesion process. As depicted in Fig. 1, *C–E*, during the 10 min incubation the platelets did not adhere when nanosheets were coated with BSA, when thrombin was treated with the thrombin inhibitor hirudin (20) before platelet addition, or when the platelets were treated with the PAR-1 receptor antagonist SCH79797 (21). Hence, platelet adhesion is clearly triggered by a pathway involving activation by thrombin.

Because thrombin also binds to GPIbα on the platelet surface (10), we assessed the extent to which such an interaction might underlie the observed process. As shown in Fig. 1, *F* and *G*, we did not observe any effect when the thrombin-GPIbα-interaction was blocked by GPIbα antibodies, consistent with the previous finding that activation via thrombin binding to GPIbα is unnoticed due to the stronger activation via PARs (10). Inhibition of the thrombin protease activity by PPACK resulted in binding and formation of filopodial extensions of a very small fraction of platelets (<2% surface coverage) without full spreading. This mode of recruitment was blocked by GPIbα antibodies. Hence, in the absence of PAR signaling, only few platelets, which are not fully spreading, are recruited by thrombin binding to GPIbα (Fig. 1, *F* and *G*). This demonstrates that in our assay the major activation pathway involves signaling via PARs.

We then sought to determine whether the major platelet integrin $\alpha_{IIb}\beta_3$, which is largely involved in most types of platelet adhesion and aggregation (22), is also required for adhesion in the nanosheet assay. This integrin is composed of the glycoproteins IIb and IIIa, the latter of which binds via its RGD binding domain to α-granule-secreted fibrinogen, fibronectin, and von Willebrand factor. Hence, we tested whether an RGDS peptide would compete with platelet-secreted, nanosheet-adsorbed proteins for binding to GPIIIa. In addition, we assessed the blocking effect of the antibody ReoPro directed against the glycoprotein IIb/IIIa receptor. As presented in Fig. S2, neither RGDS nor ReoPro reduced the number of bound platelets or seemed to abolish the formation of filopodial extensions. However, they both blocked full spreading. RGDS blocked spreading more strongly than ReoPro, indicating that other integrins containing GPIIIa may be involved as well, or that the concentration/accessibility of the ReoPro antibody

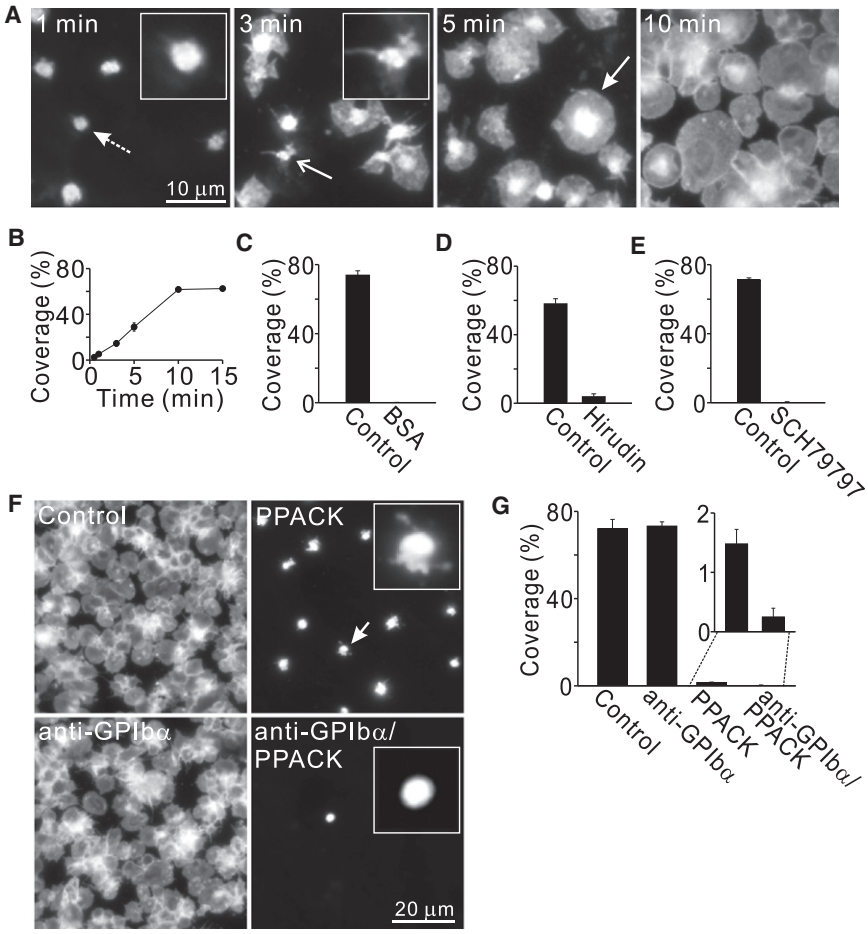

FIGURE 1 Nanosheet-adsorbed thrombin activates platelet adhesion with high specificity. (*A* and *B*) Time course of platelet adhesion. Platelets were incubated with thrombin-coated nanosheets (10 U/ml) at 37°C for various time periods (as indicated) and washed. The adsorbed platelets were imaged by fluorescence microscopy and visualized by means of the lipophilic fluorescent dye TMA-DPH. For quantification of adsorption kinetics, the area covered by platelets was determined and plotted against the incubation time. Area coverage includes all platelet stages on the pathway to full spreading. Dotted, open, and solid arrows mark an adsorbed platelet, a bound platelet with filopodial extensions, and a fully spread platelet, respectively (see also magnified views shown at different scalings). (*C*) Nanosheets were coated with 10 U/ml thrombin or thrombin was replaced by 3% BSA. The incubation time on the nanosheets was 10 min. (*D*) Nanosheets coated with 10 U/ml thrombin were incubated for 15 min at 37°C with or without 10 U/ml of the thrombin inhibitor hirudin. After two washing steps, the platelets were added to the nanosheets for a 10-min incubation. (*E*) Platelets were treated for 15 min at 37°C with or without 20 μM SCH79797, which inhibits the PAR-1 receptor for thrombin binding. The platelets were then incubated for 10 min with nanosheets coated with 10 U/ml thrombin. (*F* and *G*) Blocking of the thrombin receptor GPIbα and application of the thrombin inhibitor PPACK (which is not supposed to interfere with binding of GPIbα to thrombin). Before the platelets were exposed for 10 min to the 10 U/ml thrombin-coated nanosheets, 15-min incubations at 37°C were performed. Platelets were treated with control solutions or 10 μg/ml anti-GPIbα, and nanosheets were incubated with or without 20 μM PPACK, followed by two washing steps. (*F*) Images from the different conditions showing that anti-GPIbα alone had no effect but the combined treatment of antibody and PPACK strongly inhibited platelet adhesion. PPACK alone allowed a minor population of platelets to bind (see also magnified views); for quantification see panel *G*. Please note that in the absence of thrombin or at very low thrombin concentrations (see also Figs. 3 and 6), virtually no adhesion occurs, demonstrating that the nanosheets themselves do not activate platelets. All images are shown at arbitrary scalings. Values are given as the mean ± SE (n = 3–4 independent experiments).

is not sufficient to produce the same inhibition effect as the smaller and more highly concentrated RGDS peptide. However, the data suggest that integrin $\alpha_{IIb}\beta_3$ is the major adhesion molecule used by platelets for spreading out under these conditions.

A hallmark for platelet activation is the clustering of integrin $\alpha_{IIb}\beta_3$ (23). To determine whether clustering would also occur under our experimental conditions, we immunostained the platelets for GPIIb. As shown in Fig. S3, the staining was spotty but the signals were too blurry to clearly assess the degree of integrin clustering. Therefore, we turned to isoSTED microscopy (16), which provides a several-fold higher resolution in both the lateral and axial dimensions. This higher resolution allows for lateral resolution of the dense clusters in the plane of the membrane, and axial resolution of the basal and apical membranes, which after spreading are only a few 100 nm apart (i.e., below the resolution limit of a conventional microscope). As presented in Fig. 2, isoSTED microscopy readily resolved the two membranes and thereby allowed the analysis of cluster size and density in the adherent membrane. The integrin was highly concentrated in ~58 nm large clusters at a density of 34 clusters per μm^2, in line with our assumption that nanosheet-adsorbed thrombin is capable of triggering platelet activation. In summary, the data show that thrombin-coated nanosheets provide functionalized surfaces that can induce platelet adhesion and spreading with high specificity.

So far, the data demonstrate that thrombin-coated nanosheets specifically trigger platelet adhesion. Moreover, in 10 min and at a coating concentration of 10 U/ml, the cell spreading process is completed. We next characterized the dose-response relationship, keeping the incubation time constant at 10 min but varying the coating concentration. As shown in Fig. 3, lower coating concentrations gradually diminished adhesion, indicating that the sensitivity of the platelets varies over a wide range and/or that the greater the number of PAR receptors cleaved by thrombin, the stronger is the activation of intracellular signaling pathways.

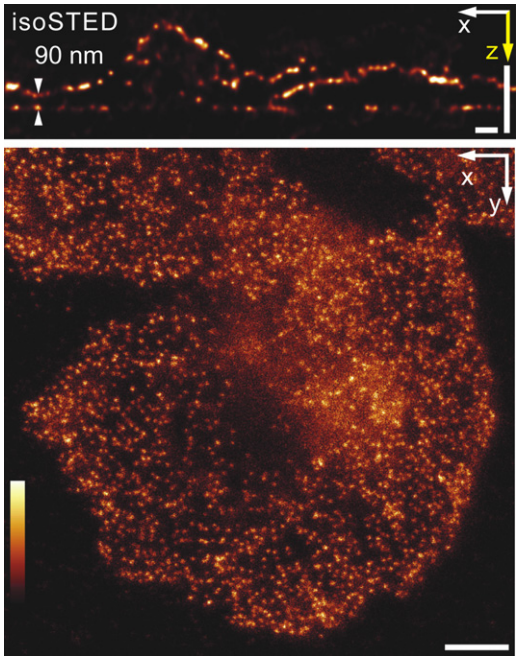

FIGURE 2 Clustering of integrin $\alpha_{IIb}\beta_3$ indicates platelet activation. After stimulation for 10 min on 10 U/ml-coated nanosheets, the platelets were fixed, immunostained with an antibody raised against GPIIb, and imaged by isoSTED microscopy. GPIIb staining reveals the distribution of the integrin complex $\alpha_{IIb}\beta_3$, which was further analyzed in the basal adherent membrane. Upper panel: An *xz* scan illustrating the microscopic separation of the apical and basal plasma membranes (scale bars: 500 nm for both the *x* and *z* directions). Lower panel: An *xy* scan from a different sample, showing basal plasma membranes recorded for visualization and analysis of the integrin $\alpha_{IIb}\beta_3$ distribution. An average cluster size of 58 ± 5 nm and cluster density of 34 ± 4 clusters per μm^2 ($n = 12$ cells) are revealed. Values are given as the mean ± SD. Scale bar: 1 μm. The look-up table illustrates intensities from 0 to 1 a.u. displayed as black and white, respectively.

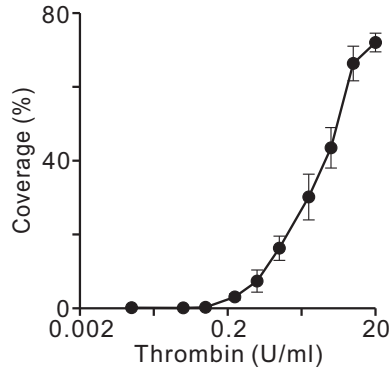

FIGURE 3 Dose-response relationship for platelet adhesion. Platelets were incubated for 10 min at 37°C with nanosheets coated with thrombin in concentrations ranging from 0.01 to 20 U/ml, and platelet area coverage was plotted against the thrombin coating concentration. Values are given as the mean ± SE ($n = 3$–7 independent experiments).

This would lead to an overall faster response of more cells, which in turn would result in larger surface coverage.

To characterize the sensitivity of the platelets in more detail, we further sought to determine the number of molecules with which a platelet establishes contact, and whether the response at low thrombin concentrations depends on the incubation time.

To obtain the number of thrombin molecules per platelet, we measured the thrombin density on the nanosheets and the size of the platelet-nanosheet contact area. For the thrombin density, we determined the amount of nanosheet adsorbed protein by measuring the adsorbed protein directly on detachable nanosheets and the loss of protein from the coating solution (for example, 0.25 U/ml would yield a value of 10.1 ng; Fig. 4 *A*). When we corrected for protein aggregation at the rim of the nanosheets (Fig. S4), we obtained a protein surface concentration of 60.1 ag/μm^2, or 4.8 ag thrombin/μm^2 taking into account the percentage of thrombin in the coating solution (7.96%; see also Fig. S5). At a molecular mass of 36,500 g/mol, this corresponds to 79 adsorbed thrombin molecules per μm^2. However, not all molecules are active, as random adsorption should shield the reactive center of a large percentage of them. To obtain the percentage of inactive molecules, we compared the proteolytic activity of free and adsorbed thrombin using a small, cleavable substrate. As presented in Fig. 4 *B*, only 29% of the maximal activity was observed after adsorption, suggesting that ~70% of the molecules are adsorbed in an orientation that does not allow the thrombins to exert their cleavage activity on the target receptor. The percentage of thrombin that cannot be reached by the PAR receptors is probably even higher, as adsorbed thrombin molecules are more accessible to a freely diffusing small substrate than to a bulky receptor in a platelet membrane. However, using this experiment as a reference, we estimate that the surface concentration of active thrombin molecules is <23 molecules per μm^2 at a coating concentration of 0.25 U/ml.

We determined the contact area of platelets using TIRF microscopy, which images the part of the platelet membrane that is in contact with the nanosheet (Fig. 5). Online recordings revealed that after they settled down to the nanosheets, the platelets immediately started to spread in the presence of thrombin (data not shown). Therefore, we settled platelets down onto thrombin-free nanosheets, allowing contact without stimulation, and simulating the starting point just before activation. The platelets were imaged under two illumination modes (Fig. 5 *A*). Using epifluorescence microscopy, we imaged all platelets present. We then recorded the same field of view by applying TIRF microscopy and illuminating only the first few 100 nm near the glass-water interface with the platelet contact area, and visualized the footprints of the same platelets observed with epifluorescence microscopy. The footprints were outlined and their size was calculated, yielding a value of 0.47 μm^2. Consequently, at a surface density of, e.g., 23 accessible thrombin molecules per μm^2, the average platelet has contact with 11 molecules. Correspondingly, using the

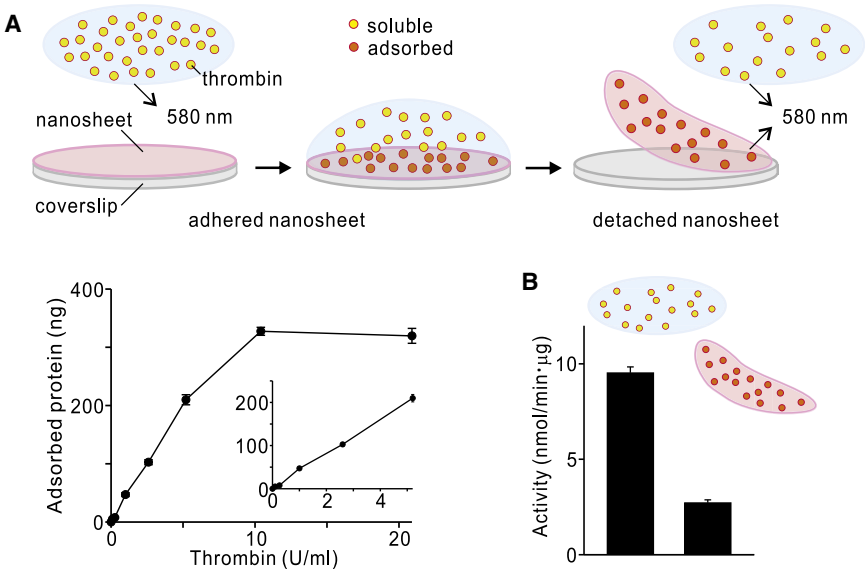

FIGURE 4 Amount of nanosheet-adsorbed protein and thrombin activity after adsorption. (*A*) Quantification of nanosheet-adsorbed protein. Detachable nanosheets were coated overnight with a fluorescently labeled thrombin solution of a protein concentration as indicated on the *x* axis of the graph. After incubation, the coating solution was collected and the nanosheets were detached from the coverslip. To determine the amount of adsorbed protein, fluorescence at 580 nm was measured, with the coating solutions (before and after coating) and detached nanosheets used as samples. Loss of protein from the coating solution was calculated (corresponding to the adsorbed protein) and averaged with the amount of adsorbed protein measured directly from the nanosheets. The averaged values were used for plotting. The graph shows averaged individual curves from several experiments, and the magnified view shows the linear range of the graph. Values are given as the mean ± SE ($n = 4$). To obtain the amount of adsorbed protein at the respective coating concentration, values were obtained from regression lines fitted to the linear ranges of the graphs from the individual experiments (e.g., for 0.25 U/ml, a value of 10.1 ng/nanosheet ($n = 4$) was obtained). (*B*) Accessibility of the reactive center from adsorbed thrombin molecules. Thrombin activity was assayed by using the cleavable chromogenic substrate N-(p-tosyl)-Gly-Pro-Arg-p-nitroanilide. A comparison of the activities of soluble and adsorbed thrombin (placing detached nanosheets into the spectrophotometer) shows that adsorption caused a decrease in activity to 29%. This suggests that thrombin adsorbs to the nanosheet in random orientations and that only 29% of the thrombin molecules have free access to the cleavable substrate.

same calculation, we obtained values of <1, 2, 4, 22, 43, and 108 molecules for 0.01, 0.05, 0.1, 0.5, 1, and 2.5 U/ml, respectively. Most likely, the actual molecule numbers are even lower, because we may have overestimated the size of the accessible thrombin fraction (Fig. 4 *B*; see above) and not all thrombin molecules in the reconstituted thrombin solution are expected to be active (only 88% of human thrombin purified from plasma is active (24), and ~10% of the activity is lost upon freezing and thawing (data not shown)). However, the data show that at a coating concentration of 0.25 U/ml, significant adhesion can be observed (Fig. 3), and that ~10 molecules are sufficient for platelet spreading in 10 min.

To determine whether the adhesion response is also time-dependent, we studied adhesion at low thrombin concentrations after 5- or 30-min incubations (Fig. 6). As presented in Fig. 6, the sensitivity for irreversible cell spreading is also time-dependent, and even <10 molecules can induce cell spreading if the incubation time is increased to 30 min.

As outlined above, the values indicating the molecule number per platelet are somewhat overestimated. On the other hand, stochastic distribution of adsorbed molecules may lead to a variable distribution of molecules per platelet, and it is possible that platelets with more than the average molecule density are preferentially activated. However, taken together, our results indicate that only a few thrombins are sufficient for platelet spreading. It is possible that only one molecule would suffice for extraordinarily long incubation times of several hours; however, this would most likely play no role under physiological conditions.

It was previously demonstrated that in solution the sole platelet activation requires a concentration that is equivalent to ~1200 thrombin molecules per platelet (6). Hence, in steady state, at most 1200 thrombin molecules bind to the entire surface of one platelet. However, as outlined in the Introduction, the number of acting molecules cannot be determined because it is unclear how many free thrombins are in equilibrium with PAR-receptor-bound thrombins. In this study, we defined the number required for platelet adhesion on a surface with immobilized thrombin molecules. In fact, <10 molecules are sufficient, and although this is not directly comparable to the situation in solution, it is much less than one might have expected.

There are three possible explanations for this high sensitivity. First, as in vivo, in our assay the reaction occurs at a thrombin-platelet interface at which thrombin molecules and platelet receptors orient like in a solid-state interaction. The entropy change for the thrombin-platelet receptor complex formation is minimized in this configuration, resulting in an acceleration of the reaction kinetics. This is in line with the previous observation that another cell activation mechanism occurring in the solid-state configuration had a similarly low sensitivity of 10 antigen molecules required for mature immunological synapse formation (25). Second, thrombin is a protease that is capable of activating more than one receptor irreversibly. At first glance it seems odd that a receptor can be irreversibly activated, and it is unclear why PARs have evolved in this direction. However, the mechanism allows one immobilized thrombin to activate several receptors quickly, one after another. This

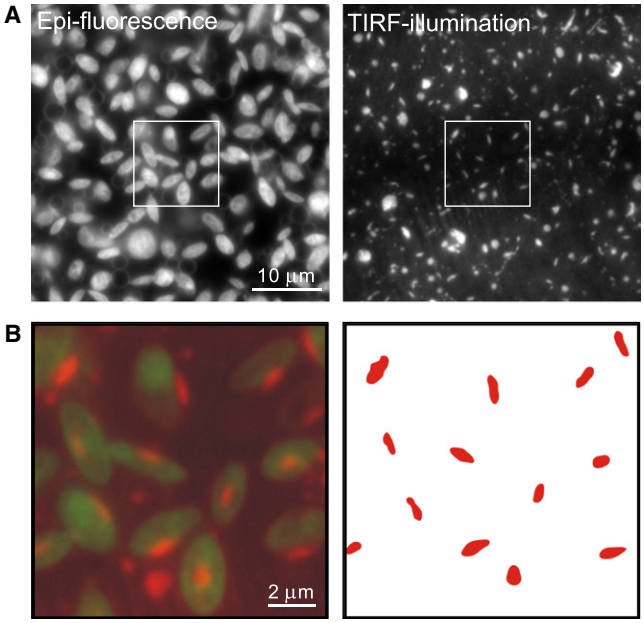

FIGURE 5 Platelet footprints imaged by TIRF microscopy. (*A*) Platelets settled down onto BSA-coated coverslips were visualized with the membrane staining dye FM1-43 and imaged by epifluorescence (*left*) and TIRF microscopy (*right*). (*B*) Left: Magnified view from the overlay of the epifluorescence image (*green*) and the TIRF micrograph (*red*). Nonactivated platelets and their corresponding footprints were identified, outlined, and further processed (*right panel*). Determination of their average size yielded a value of 0.47 ± 0.04 μm^2 (mean ± SE, $n = 3$ independent experiments; 181–413 footprints were analyzed for each experiment).

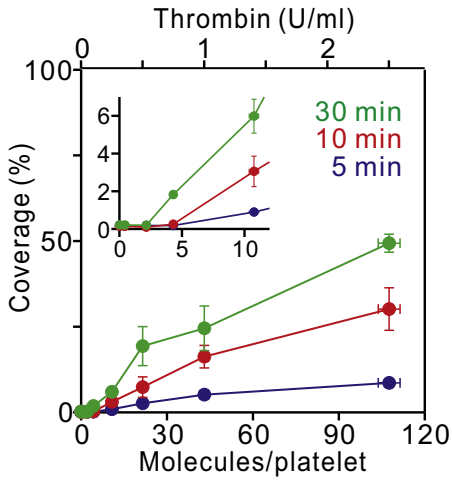

FIGURE 6 Platelet sensitivity for irreversible adhesion. Platelets were incubated for 5 min (*blue line*) or 30 min (*green line*) at 37°C with nanosheets coated with thrombin in concentrations ranging from 0.01 to 2.5 U/ml, and surface coverage was plotted against the thrombin coating concentration. For comparison, data from Fig. 3 are also shown (10 min incubations, *red line*). For plotting, the U/ml values (upper *x* axis) were converted into active thrombin molecules per platelet contact area (lower *x* axis; for explanation see text). Values are given as the mean ± SE (n = 3–7 independent experiments for platelet adhesion, and $n = 4$ for determination of molecule number).

is not possible in solution, because after cleavage thrombin is released into the solution, diffusing away from the membrane. Third, 10 immobilized molecules acting on a small membrane patch (the platelet contact site) might trigger locally higher signals than would 10 soluble molecules stochastically distributed over the cell membrane. For these reasons, we suggest that immobilization of the proteolytically active thrombin in conjunction with the PAR reaction pathway can maximize the effect of a few signaling molecules, resulting in a higher sensitivity.

Hence, although they depend on the same key players, interactions in solution or in the solid state involve different steps that become rate-limiting for the overall reaction kinetics. This has implications for the interpretation of in vitro coagulation tests. Recently, Mann et al. (26) pointed out that all in vitro coagulation tests are limited due to the absence of contributing vasculature and surrounding tissue, which would mediate the solid-state interaction described here. Given that in vivo testing in humans is precluded because of the high pathophysiological risks involved, the described system could be useful for generating more-physiological assay conditions to evaluate the effects of antithrombotic drugs or the antithrombotic properties of the surfaces of artificial organs.

In summary, our findings demonstrate that only a few signaling molecules are sufficient to achieve irreversible platelet adhesion. Similarly, 10 molecules activate T-cell immunological synapse formation (25). This parallel may indicate another biological significance. Sensory systems are able to detect even single molecules (25,27) or photons (28), but false registrations are tolerable when individual signals are integrated and neuronally processed. This is different for irreversible cell activation, in which case single-molecule responses can generate undesired effects if the signaling molecule accidentally marks a site at which the cellular function is not required or would even be harmful. Hence, it is possible that nature has balanced these systems to minimize false activation while still allowing for the highest sensitivity, resulting in the requirement of only a few signaling molecules per cell.

SUPPORTING MATERIAL

Five figures are available at http://www.biophysj.org/biophysj/supplemental/S0006-3495(11)00305-5.

We thank Dr. Yasuo Ikeda (Waseda University, Tokyo, Japan) and Dr. Silvio Rizzoli (European Neuroscience Institute, Göttingen, Germany) for valuable discussions, Dr. Stefan W. Hell (MPI for Biophysical Chemistry, Göttingen, Germany) for support and comments on the manuscript, and Dr. Tobias Lamkemeyer (CECAD, University of Cologne, Cologne, Germany) for the proteomic analysis.

Y.O. is a research fellow of the Mitsubishi Pharma Research Foundation (2009), the Alexander von Humboldt Foundation (2010), and the Japan Society for the Promotion of Science (Postdoctoral Fellowships for Research Abroad 2011). A.E. was supported by a grant from the Deutsche Forschungsgemeinschaft (SFB 755), and S.T. was supported in part by the

High-Tech Research Center Project (Waseda University) and a grant-in-aid for scientific research ((B) 21300181) from MEXT.

REFERENCES

1. Davis, M. M., M. Krogsgaard, …, Q. J. Li. 2007. T cells as a self-referential, sensory organ. *Annu. Rev. Immunol.* 25:681–695.
2. Kaupp, U. B. 2010. Olfactory signalling in vertebrates and insects: differences and commonalities. *Nat. Rev. Neurosci.* 11:188–200.
3. Ueda, M., and T. Shibata. 2007. Stochastic signal processing and transduction in chemotactic response of eukaryotic cells. *Biophys. J.* 93: 11–20.
4. Fuster, V., L. Badimon, …, J. H. Chesebro. 1992. The pathogenesis of coronary artery disease and the acute coronary syndromes (1). *N. Engl. J. Med.* 326:242–250.
5. Fuster, V., L. Badimon, …, J. H. Chesebro. 1992. The pathogenesis of coronary artery disease and the acute coronary syndromes (2). *N. Engl. J. Med.* 326:310–318.
6. Brummel, K. E., S. G. Paradis, …, K. G. Mann. 2002. Thrombin functions during tissue factor-induced blood coagulation. *Blood.* 100: 148–152.
7. Jackson, S. P., W. S. Nesbitt, and E. Westein. 2009. Dynamics of platelet thrombus formation. *J. Thromb. Haemost.* 7 (*Suppl 1*):17–20.
8. Bar-Shavit, R., A. Eldor, and I. Vlodavsky. 1989. Binding of thrombin to subendothelial extracellular matrix. Protection and expression of functional properties. *J. Clin. Invest.* 84:1096–1104.
9. Dardik, R., D. Varon, …, A. Inbal. 2000. Recombinant fragment of von Willebrand factor AR545C inhibits platelet binding to thrombin and platelet adhesion to thrombin-treated endothelial cells. *Br. J. Haematol.* 109:512–518.
10. Adam, F., M. C. Guillin, and M. Jandrot-Perrus. 2003. Glycoprotein Ib-mediated platelet activation. A signalling pathway triggered by thrombin. *Eur. J. Biochem.* 270:2959–2970.
11. Coughlin, S. R. 2000. Thrombin signalling and protease-activated receptors. *Nature.* 407:258–264.
12. Aquino, D., A. Schönle, …, A. Egner. 2011. Two-color nanoscopy of three-dimensional volumes by 4Pi detection of stochastically switched fluorophores. *Nat. Methods.*, March 13. [Epub ahead of print].
13. Okamura, Y., K. Kabata, …, S. Takeoka. 2009. Free-standing biodegradable poly(lactic acid) nanosheet for sealing operations in surgery. *Adv. Mater.* 21:4388–4392.
14. Harris, L. R., M. A. Churchward, …, J. R. Coorssen. 2007. Assessing detection methods for gel-based proteomic analyses. *J. Proteome Res.* 6:1418–1425.
15. Luo, S., N. B. Wehr, and R. L. Levine. 2006. Quantitation of protein on gels and blots by infrared fluorescence of Coomassie blue and Fast Green. *Anal. Biochem.* 350:233–238.
16. Schmidt, R., C. A. Wurm, …, S. W. Hell. 2008. Spherical nanosized focal spot unravels the interior of cells. *Nat. Methods.* 5:539–544.
17. Staudt, T., M. C. Lang, …, S. W. Hell. 2007. 2,2′-thiodiethanol: a new water soluble mounting medium for high resolution optical microscopy. *Microsc. Res. Tech.* 70:1–9.
18. Ullal, C. K., R. Schmidt, …, A. Egner. 2009. Block copolymer nanostructures mapped by far-field optics. *Nano Lett.* 9:2497–2500.
19. Richardson, W. H. 1972. Bayesian-based iterative method of image restoration. *J. Opt. Soc. Am.* 62:55–59.
20. Warkentin, T. E. 2004. Bivalent direct thrombin inhibitors: hirudin and bivalirudin. *Best Pract. Res. Clin. Haematol.* 17:105–125.
21. Ahn, H. S., C. Foster, …, M. Graziano. 2000. Inhibition of cellular action of thrombin by N3-cyclopropyl-7-[[4-(1-methylethyl)phenyl] methyl]-7H-pyrrolo[3, 2-f]quinazoline-1,3-diamine (SCH 79797), a nonpeptide thrombin receptor antagonist. *Biochem. Pharmacol.* 60:1425–1434.
22. Shattil, S. J., and P. J. Newman. 2004. Integrins: dynamic scaffolds for adhesion and signaling in platelets. *Blood.* 104:1606–1615.
23. Isenberg, W. M., R. P. McEver, …, D. F. Bainton. 1987. The platelet fibrinogen receptor: an immunogold-surface replica study of agonist-induced ligand binding and receptor clustering. *J. Cell Biol.* 104:1655–1663.
24. Fenton, 2nd, J. W., M. J. Fasco, and A. B. Stackrow. 1977. Human thrombins. Production, evaluation, and properties of α-thrombin. *J. Biol. Chem.* 252:3587–3598.
25. Irvine, D. J., M. A. Purbhoo, …, M. M. Davis. 2002. Direct observation of ligand recognition by T cells. *Nature.* 419:845–849.
26. Mann, K. G., T. Orfeo, …, K. Brummel-Ziedins. 2009. Blood coagulation dynamics in haemostasis. *Hamostaseologie.* 29:7–16.
27. Gutiérrez, A., S. Marco, editors. Biologically Inspired Signal Processing. Springer Verlag, Heidelberg. *In* The Sensitivity of the Insect Nose: The Example of Bombyx Mori. 45–52.
28. Baylor, D. 1996. How photons start vision. *Proc. Natl. Acad. Sci. USA.* 93:560–565.